Nuclear Science and Techniques **23** (2012) 139–143

Preparation and characterization of graphene nanoribbons

ZHANG Huifang[1,2] LIU min[1,2] YAN Long[1,*] YU Guojun[1] ZHOU Xingtai[1]

[1]*Shanghai Institute of Applied Physics, Chinese Academy of Science，shanghai 201800,China*

[2]*Graduate School of the Chinese Academy of Sciences, Beijing 100049, China*

Abstract Graphene nanoribbons (GNRs) have been synthesized by unzipping oxidized multiwalled carbon nanotubes. The thickness of the GNRs synthesized is ranged from mono-layer to four layers. The morphology of prepared GNRs is strongly dependent on structure and defects of the MWCNTs. The synchrotron radiation X-ray diffractions show the $d_{(002)}$ spacing of the GNRs decreases with the increase of the annealing temperature. This may be caused by the removing of water molecules and oxygen-containing functional groups in the GNRs.

Key words Graphene Nanoribbons, Transmission electron microscope (TEM), Atomic force microscope (AFM), Raman spectrum, Synchrotron radiation X-ray diffraction

1 Introduction

Graphene, a novel two-dimensional graphite material, has attracted tremendous attention because of their unique structure, excellent electronic and mechanical properties, and promising applications in carbon-based electronic, composite materials, etc[1-6]. Graphene nanoribbons (GNRs) are elongated strips of graphene with widths from a few to tens of nanometers. GNRs of less than 10 nm width, due to the quantum confinement and edge effects, are semiconductors, and the energy gaps of GNRs can be easily engineered by varying the width[7-9]. Also, GNRs have unusual physical properties, such as a half metallic nature, a spin-polarized ground state in zigzag shaped GNRs and enhanced excitonic effects[7-9], which attracted increasing research activities in GNR synthesis.

GNRs have been synthesized by lithography and chemical etching methods[7,10-14]. Recently, a new method for GNR synthesis, i.e., longitudinal unzipping of multiwalled carbon nanotubes (MWCNTs), was reported[15-17]. The mechanism of this method is to unzip MWCNTs by breaking the carbon-carbon bonds in MWCNTs[18,19]. GNRs of various shapes can thus be synthesized in a complex process of chemical oxidization.

Nevertheless, intrinsic structures of the GNRs shall be clarified. In this work, GNRs in different shapes were synthesized, and structures of the GNRs annealed at different temperatures were analyzed by synchrotron radiation X-ray diffraction (XRD) at Shanghai Synchrotron Radiation Facility (SSRF).

2 Experimental

MWCNTs in purity of 98%, in diameters of 60–100 nm, were produced by Shenzhen Nanotech Port Co. Ltd. H_2SO_4 and $KMnO_4$, all of analytical degree, were from Sinopharm Chemical Reagent Co. Ltd. Deionized water was used for all the chemical procedures.

In a typical procedure, MWCNTs were suspended in concentrated H_2SO_4 for 8–10 h and treated with 500 wt% $KMnO_4$. The H_2SO_4 helped exfoliating the MWCNTs into graphene structures. The reaction mixture was stirred at room temperature for 1 h and heated to 55ºC–70ºC for 8 h. When all the $KMnO_4$ was consumed, the reaction mixture was quenched by adding ice containing a small amount of hydrogen peroxide (H_2O_2). The solution was filtered

---

Supported by National Basic Research Program of China (Grant No. 2010CB832903) and National Natural Science Foundation of China (No.50902147)

* Corresponding author. *E-mail address:* yanlong@sinap.ac.cn

Received date: 2011-03-14

with a polytetrafluoroethylene (PTFE) membrane of 0.2-μm pore size. The solid residuals were washed by acidic water followed by ethanol. The as-synthesized GRNs are stable in alcohol solution, as shown in Fig.1a.

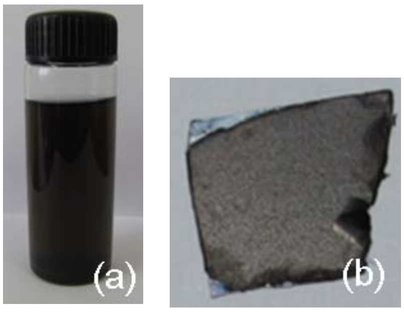

Fig.1 Photographs of the prepared GNR alcohol solution (a) and the graphene film on a silicon substrate (b).

The prepared GNRs were characterized by atomic force microscope (AFM,), transmission electron microscope, Raman spectroscopy, and synchrotron radiation XRD. For the XRD measurement, a GNR film prepared by a vacuum filtration method[20] was transferred to a silicon substrate, as shown in Fig.1b.

AFM images were obtained by SPA-400 scanning probe microscope in tapping mode. Field emission JEOL JEM-2010F TEM at 200 kV was observed structures of the prepared GNRs. Raman spectroscopy was carried out using a Jobin Yvon LabRAM HR800 Raman microscope, excited by a 632.8 nm laser. Synchrotron radiation XRD measurement was performed at Beamline 14B of SSRF, using the X-ray in wavelength of 0.12398 nm.

3 Results and discussion

The TEM image in Fig.2a shows, indicated by the arrows, that the MWCNTs are completely unzipped and thin GNRs are formed in different shapes and thicknesses. Figs.2b shows the thick GNRs, caused possibly by accumulation of unzipped tubes. Figs.2c and 2d show that the some tubes are partly unzipped, as indicated by the arrows. This is because that some tubes were not completely oxidized by $KMnO_4$, and in the oxidized exfoliation process, due to defects in the MWCNTs, some GNR fragments could be peeled off from oxidized MWCNTs (arrow 8 in Fig.2d).

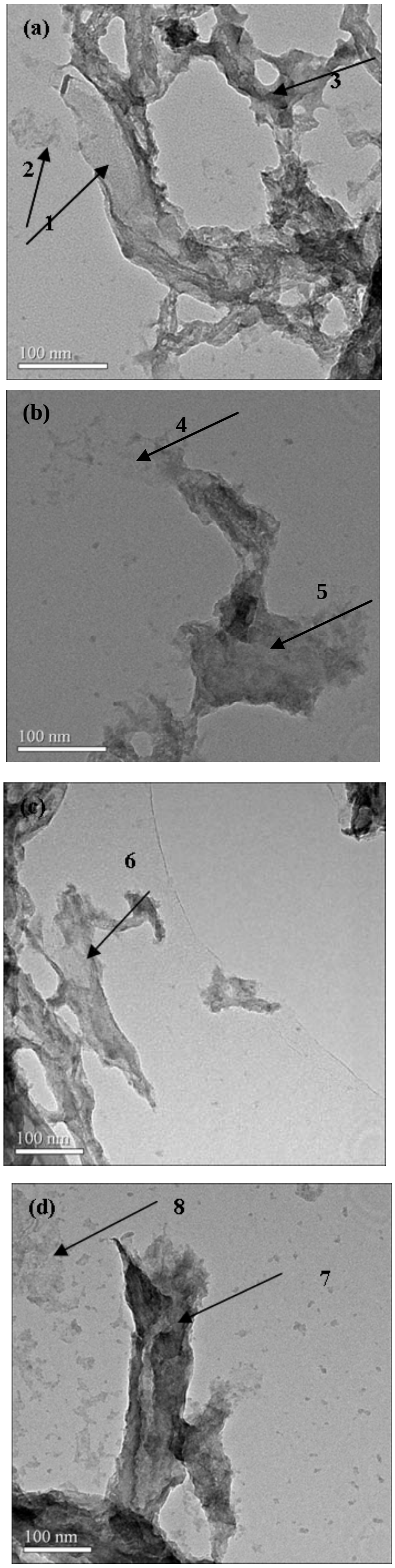

Fig.2 TEM images of the as-prepared GNRs. (a) and (b) completely unzipped, (c) and (d) partially unzipped.

The AFM images (Fig.3) revealed that topographic height of the GNRs ranged 1−4 nm. These are corresponding to their thickness range from mono-layer to four layers. Their morphologies, however, are diverse. Some GNRs are of hundreds of nanometers in size (Figs.3a and 3b). Some GNRs have smooth edges (Fig.3a), indicating that the MWCNT unzipping proceeded exactly along the crystallographic orientations of the tubes; while some GNRs have rough edges (Fig.3b), which might be cause by random irregular distribution of defects in MWCNTs so that the unzipping did not proceed along the tube crystallographic orientations exactly. Fig.4c shows some GNR fragments of 10–50 nm, which is in agreement with our TEM observation. In Fig.3d (the arrows) the island-like structures are nano carbon particles[21]. From the TEM and AFM observations, the GNR morphology is strongly dependent on structures and defects of the MWCNTs.

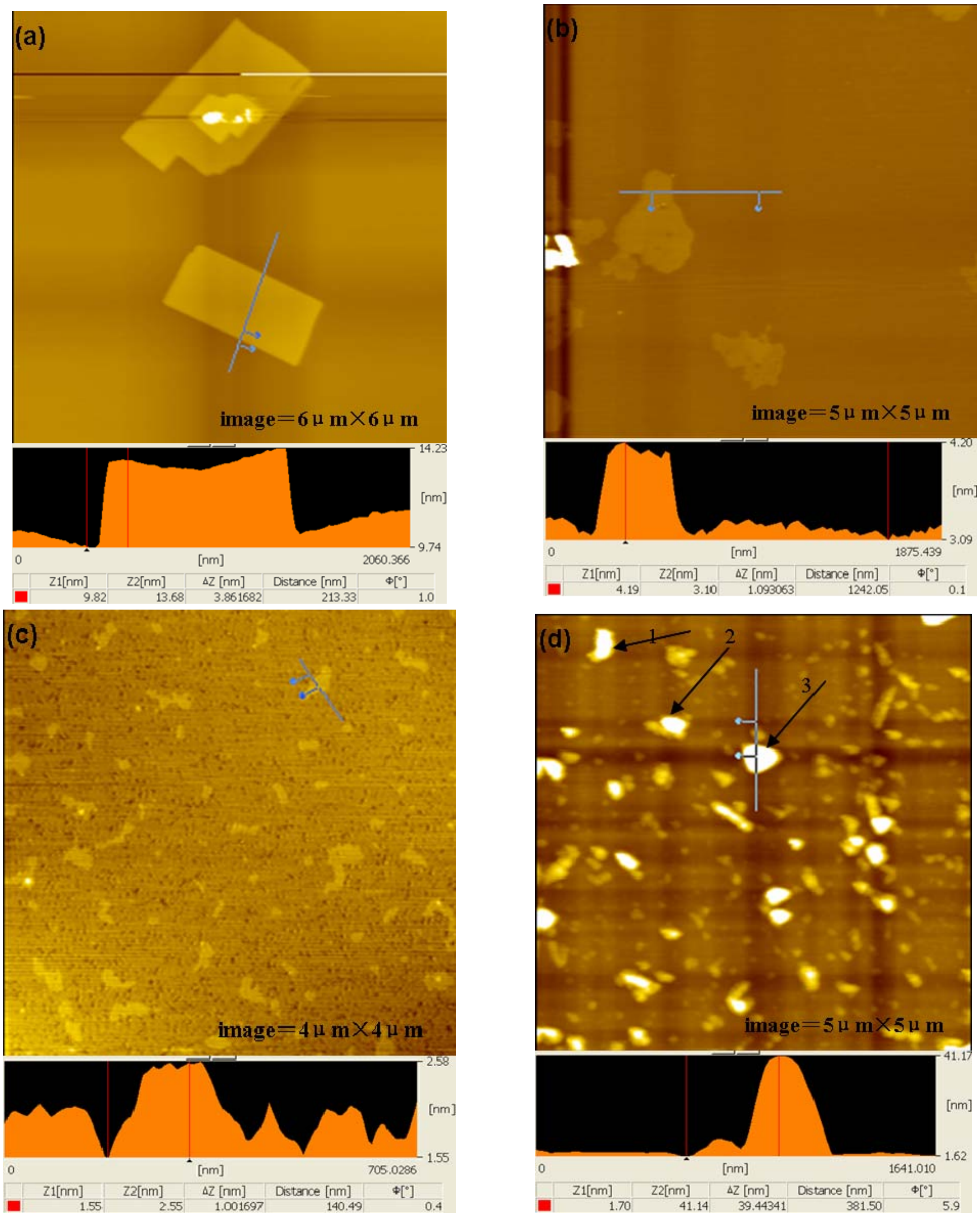

Fig.3 AFM images of the GNRs. The height profiles along the line in the images show the width and thickness of the GNRs. (a) and (b) GNRs in hundreds of nanometers, (c) GNR fragments of 10–50 nm and (d) island-like structures.

In Fig.4, the Raman spectra of the MWCNTs and the prepared GNRs comprise two broad peaks: the G-band at ~1580 cm^{-1} attributed to vibration of sp^2 bonded carbon atoms in a two-dimensional hexagonal lattice, and the D-band at ~1350 cm^{-1} attributed to vibration of carbon atoms with disordered graphite. From Fig.4, it can be seen that both the G- and D-bands are located at a higher frequency in the GNRs than those in the MWCNTs. That is, a blue Raman shift occurs after the MWCNTs are transformed to the GNRs. The blue shift are ascribed to the presence of carbon-carbon double bonds[22]. After the MWCNTs are unzipped by chemical oxidation, the formed GNRs have an amount of edges and oxygen-containing functional groups (-OH, -C=O, -CHO, -COOH). These cause the obvious increase of carbon-carbon double bonds. Therefore, the blue shift of the Raman spectra of GNRs relative to that of the MWCNTs is usually observed.

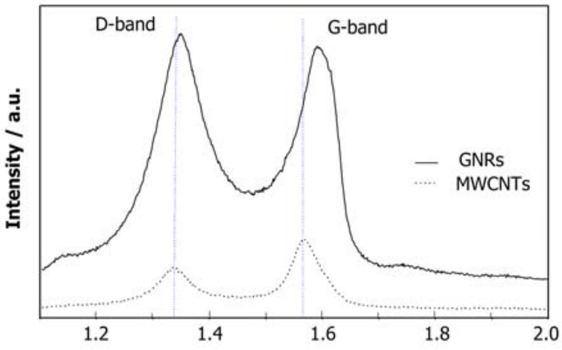

Fig.4 Raman spectra of the MWCNTs and the GNRs.

In order to investigate structure of the prepared GNRs, XRD analysis of the samples annealed at different temperatures was performed on Beamline 14B at SSRF. Fig.5 shows the synchrotron radiation XRD patterns of a GNR film at different temperatures. The distinct main diffraction peak at around 20.6° is corresponding to a $d_{(002)}$ spacing of GNRs. The diffraction peaks are fairly broad, indicating that the prepared GNRs are in nanometer size. This is consistent with our TEM and AFM observations. From the XRD patterns, the $d_{(002)}$ spacing of GNRs can be estimated at 3.475 Å at room temperature, larger than that of graphite (3.354 Å). The big $d_{(002)}$ spacing suggests some foreign molecules in the GNRs. Annealing is an efficient way to exclude foreign molecules in the GNRs[23]. It can be seen that the main diffraction peak of GNRs shifts to big diffraction angles as the annealing temperature increases. The $d_{(002)}$ spacing of GNRs can be calculated as 3.468, 3.468, 3.468 and 3.429Å at 100ºC, 200ºC, 300ºC and 430ºC, respectively. From room temperature to 100ºC, the $d_{(002)}$ spacing of GNRs has an obvious decrease (from 3.475 Å to 3.468 Å). This is ascribed to desorption of water molecules in the GNRs. At 100ºC–300ºC, the $d_{(002)}$ spacing of GNRs changes little, because most of the water molecules are desorbed at 100ºC. At 430ºC, the $d_{(002)}$ spacing is further reduced, possibly due to removing of oxygen-containing functional groups at high temperature. As mentioned, some oxygen-containing functional groups in the GNRs are confirmed by the Raman spectrum of the GNRs. In addition, with increasing temperatures, a small diffraction peak appears at around 2θ=25°. This may be caused by impurities. According to the energy dispersive X-ray spectrum, the GNRs contain C, Na, O, S and Cl. At high annealing temperatures, the impurities may become gradually crystallized, hence the small diffraction peaks at high temperatures.

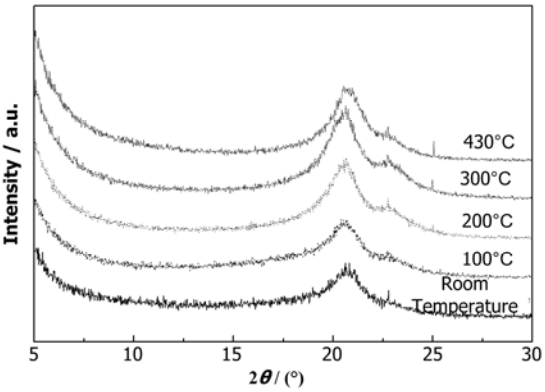

Fig.5 Synchrotron radiation in-situ X-ray diffraction.

4 Conclusion

We have fabricated GNRs by unzipping oxidized MWCNTs. The thickness of the GNRs is distributed in the range between mono-layer to four layers. The sizes of the GNRs are strongly dependent on structures and defects of the MWCNTs. The Raman and synchrotron radiation in-situ X-ray diffraction results indicate that the GNRs contain water molecules and oxygen-containing functional groups, which can be removed by annealing at high temperature.

References

1 Novoselov K S, Geim A K, Morozov S V, *et al*. Science, 2004, **306:** 666−669.

2 Westervelt R M, Science, 2008, **320:** 324–325.

3 Li X L, Wang X R, Zhang L, *et al*. Science, 2008, **319:** 1229–1232.

4 Schedin F, Geim A K, Morozov S V, *et al*. Nat Mater, 2007, **6:** 652–655.

5 Wang X, Zhi L J, Mullen K.Nano Lett, 2008, **8:** 323–327.

6 Stankovich S, Dikin D A, Geoffrey H B D, *et al*. Nature, 2006, **442:** 282–286.

7 Chen Z H, Lin Y M, Michael J R, *et al*. Phys E, 2007, **40:** 228–232.

8 Brey L, Fertig H A. Phys Rev B, 2006, **73:** 235411–35415.

9 Barone V, Hod O, Gustavo E S. Nano Lett, 2006, **6:** 2748–2754.

10 Levente T, Gergely D, Philippe L, *et al*. 2008, **3:** 397–401.

11 Melinda Y H, Barbaros O, Zhang Y B, *et al*. Rev Lett, 2007, **98:** 206805–206808.

12 Sujit S D, Douglas R S, Samuel M K, *et al*. Nano Lett, 2008, **8:** 1912–1915.

13 Ci L J, Xu Z P, Wang L L, *et al*. Nano Res, 2008, **1:** 116–122.

14 Campos L C, Manfrinato V R, Javier D S, *et al*. Nano Lett, 2009, **9:** 2600–2604.

15 Dmitry V K, Amanda L H, Alexander S, *et al*. Nat Lett, 2009, **458:** 872–876.

16 Jiao L Y, Zhang L, Wang X R, *et al*. Nat Lett, 2009, **458:** 877–880.

17 Abraham G C, Fernando J R, Jessica C D, *et al*. Nano Lett, 2009, **9:** 1527–1533.

18 Li J L, Konstantin N K, Michael J M, *et al*. Phys Rev Lett, 2006, **96:** 176101–176104.

19 Pulickel M A, Boris I Y, Nature, 2006, **441:** 818–819.

20 Goki EDA, Glovanni F, Manish C. Nat Nanotech, 2008, **3:** 270–274.

21 Franco C, Giuseppe C, Giacomo P, *et al*. Carbon, 2010, **48:** 2596–2602.

22 Ferrari A C, Robertson J. Phys Rev B, 2000, **61:** 14095–14107.

23 Becerril H A, Mao J, *et al*. ACS Nano, 2008, **2:** 463–470.